A. KOUTSOMICHALIS, N. VAXEVANIDIS, G. PETROPOULOS, E. XATZAKI, A. MOURLAS, S. ANTONIOU

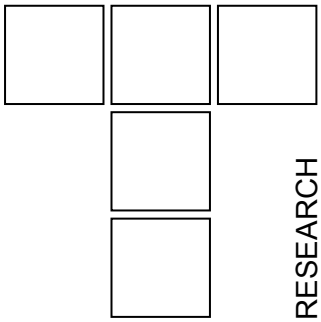

Tribological Coatings for Aerospace Applications and the Case of WC-Co Plasma Spray Coatings

Friction and wear requirements in aerospace systems are dictated by life limiting problems. One challenge is the broad range of contact stresses and sliding speeds for various movable devices. Another challenge is the extreme operation conditions; in particular an aircraft suffers periodical humidity changes depending on the altitude, broad temperature range, abrasive wear by electrostatically attracted dust. This paper discusses conventional WC–12% Co tribological coating deposited by atmospheric plasma spraying. Friction and wear characteristics were analysed using sliding friction tests (pin-on-disc apparatus). Four different test loads were used in order to examine the influence of contact stress on tribological behaviour. From the experimental data obtained plots of the variation of coefficient of friction and the wear rate with sliding distance were constructed. The tensile behaviour of the coated material as well as the corrosion resistance of coated and uncoated specinens was also examined. Having high hardness and good adhesion with the substrate the sprayed coating exhibits satisfactory wear resistance.

Keywords: *plasma sprayed WC-Co, aerospace tribological coatings, mechanical properties, wear behaviour*

1 INTRODUCTION

1.1 Plasma sprayed coatings in aerospace applications

Life-limiting parameters of aerospace systems include friction and wear in various devices along with extreme operating conditions including humidity variations with altitude changes and broad temperature ranges. Mechanical and endurance requirements of aerospace applications dictate new wear-reduction technologies demanding new materials and advanced technologies. Tribological coatings are typically exposed to high surface pressures and sliding velocities, and therefore require sufficiently good adhesion and thermal stability in order to perform well. Low friction materials usually possess friction coefficients below 0.1 in the presence of liquid lubrication, and from 0.3 down to 0.08 under boundary layer and dry friction conditions. Materials with friction coefficients exceeding 0.3 usually find tribological application as brake pads, etc. The operational parameters of anti-friction materials span a wide range: sliding speeds between 0.001 m/s and 300 m/s, contact pressures from 0.001 MPa to above 1500 MPa, and temperatures from cryogenic up to and above 1000°C.

Plasma sprayed deposition of abrasive and abradable coatings are commonly used in aerospace applications and research is focused on both their wear characteristics and degradation mechanisms. The development of vacuum deposition methods enabled composite coatings used in high temperature space lubrication coatings such as the NASA PS-200 series coatings produced by plasma spraying which consisted of BaF_2/CaF_2 lubricant, silver lubricant and binder and Cr_3C_2 support [1].

Composite coatings can either be transition-metal dichalcogenides (MoS_2, WS_2, $NbSe_2$) which

A. Koutsomichalis[1], N. Vaxevanidis[2], G. Petropoulos[3], E. Xatzaki[1], A. Mourlas[4], S. Antoniou[4]
[1] Aerospace Engineering Dept., Hellenic Air Force Academy, Dekelia Air-Force Base, 1010 Athens, Greece; e-mail:akouts@hafa.gr
[2] Dept. of Mechanical Engineering Educators, School of Pedagogical & Technological Education (ASPETE), 141 21 N. Heraklion, Athens, Greece; e-mail: vaxev@central.ntua.gr
[3] Department of Mechanical and Industrial Engineering, University of Thessaly, Pedion Areos, 38334 Volos, Greece; e-mail: gpetrop@uth.gr
[4] Laboratory of I.C.E. and Tribology, Technological Education Institute of Piraeus, Egaleo, Greece

are applied as powders mixed with various organic and inorganic binders normally deposited by spray and vacuum deposition methods.

Vacuum deposition also provided a variety of advanced hard coatings for wear protection [2,3], which are currently expanding toward aerospace applications due to the endurance requirement. Alternative tribological material for aerospace tribological applications is diamond-like carbon (DLC), which has high hardness, low friction and low wear. The use of two-phase carbide/DLC nanocomposites is reported to create problems due to DLC graphitization in friction contacts and the associated increase of friction coefficient in the high-vacuum environment [4,5].

Conventional double-layer thermally sprayed coating system is currently applied to in service components by some of the major aeroengine manufacturers. A metallic interlayer coating is applied onto the substrate by plasma spraying, and provides a base onto which a further dry film lubricant (DFL) layer is applied.

This paper discusses WC–12% Co coating deposited by atmospheric plasma spraying. Friction and wear characteristics were analysed using sliding friction tests (pin-on-disc apparatus). Four different test loads were used in order to examine the influence of contact stress on tribological behaviour. From the experimental data obtained plots of the variation of coefficient of friction were constructed and possible wear mechanisms were investigated. The tensile behaviour of the coated material as well as the corrosion resistance of coated and uncoated specinens was also examined. Having high hardness and good adhesion with the substrate the sprayed coating exhibits satisfactory wear resistance.

2 EXPERIMENTAL

WC-Co powder (12 wt. % Co) with particle grain sizes of 45-100 μm type (Sulzer-Metco 71NS) was deposited on the surface of structural steel CK60 specimens having a composition of 0.60% wt C, 0.40% wt Si, 0.75% wt Mn, 0.035% wt P and 0.035% wt S. Tensile and corrosion specimens had dimensions 130 x 90 x 2.1 mm^3, while flat circular test pieces, approximately 38 mm in diameter and 10 mm thick, were cut-off for wear tests. All specimens were grit blasted using coarse alumina. Ultrasonic cleaning in alcohol followed by hot air drying served to remove oil and grit residues. Spraying was performed within a period of 10 min following sandblasting.

Plasma spraying was carried out using a Metco 7MB gun. The spraying conditions are listed in table 1. Powder was heated for two hours in a furnace at 70° C prior to spraying, in order to eliminate moisture and optimize flow characteristics.

WC-Co coating was deposited on both sides of the flat specimens in equal thicknesses as indicated in table 2 in order to enable balanced loading during the tensile test. Circular test pieces were sprayed to an average coating thickness of 450 μm. The microstructure of the coated samples was observed under a metallographic microscope (Leica DMR) with image analysis software (Image Pro). Brentano diffractometer with CuKα radiation and a graphite monochromator was used for XRD and full spectrum scanning (20^o– 100^o) was applied.

Table 1. Spraying parameters

Plasma gases		
Pressure (psi)	Primary gas, nitrogen (N_2): 100 Secondary gas, Hydrogen (H_2): 50	
Flow (Scfm)	Primary gas, nitrogen (N_2): 75 Secondary gas, Hydrogen (H_2): 15 ± 5	
Power		
Current (A)	400	
Voltage (V)	50-55	
Powder feed		
Meter Wheel speed (rpm)		25
Flow rate (ft^3/hr)		50
Spraying conditions		
Distance (mm)		76
Spray rate (kg/h)		4.99
Efficiency		70%
Deposition rate (kg/hr)		3.5 kg/hr

Table 2. Coating thickness

sample	Thickness per side (μm)
A	72
B	432
C	203
D	356
E	152

The corrosion behaviour of coated and uncoated specimens was examined in a 0.5 M NaCl solution (pH 1) at 20^oC by measuring the potential of the immersed specimen in the solution vs. standard calomel electrode as a function of immersion time. For the evaluation of friction and wear characteristics sliding friction tests were performed (according to ASTM G 99-05 standard) on a state-of-the-art CSEM pin-on-disc apparatus properly modified to accommodate pins made of: (a) titanium carbonitride (TiCN, type IC 3028) and (b) TiCN+TiN+Al_2O_3 (type IC 9025). Three normal loads were selected, namely 10N, 5N, 3N and 1N. All tests were conducted at 16 mm track radius and with constant linear speed 0.6 m/s. A photograph of the tribometer used is shown in Figure 1.

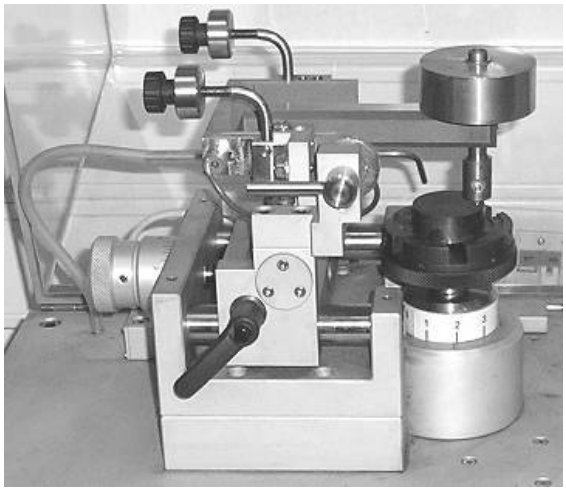

Figure 1. Photograph of the tribometer used

3 RESULTS AND DISCUSSION

Figure 2 shows the cross-sectional microstructure of the WC-Co coating produced by the atmospheric plasma spray. The coating presents a laminar microstructural morphology, typical of the spraying process. The typical morphology of the cermet coating reveals a lamellar structure with some cavities. The microstructure of plasma sprayed coatings is described as a build-up of lenticularly shaped flattened particles with thick mid sections. This results from powder being injected into hot plasma which melts the particles and accelerates them to splat onto the substrate. Molten particles solidify at high cooling rates thus preventing excessive liquid drop flow. The coating - substrate interface was wavy, the hump heights at the interface being occasionally larger than the initial substrate roughness. The coating is characterized by the presence of rather equidimensional pores. In quantitative terms, the porosity of the coating was measured by image analysis and was found to be equal to 3%. The roughness of the coating free surface was rather high (R_a=8.2 μm).

The lamellar structure is formed by the flattening of molten particles upon impact on the substrate surface forming a pancake morphology. A parameter which is used to compare droplet spreading is known as the Madjeski parameter [13]

$$\Phi_m = \frac{d}{D} = \left(\frac{2}{D}\right)\left(\frac{A}{\pi}\right)^{1/2} \qquad (1)$$

where D is the initial diameter of the molten particle, d is the splat diameter and A is the are covered by the splat. The Madjeski parameter (Φ_m) of the coating was calculated equal to 0.4.

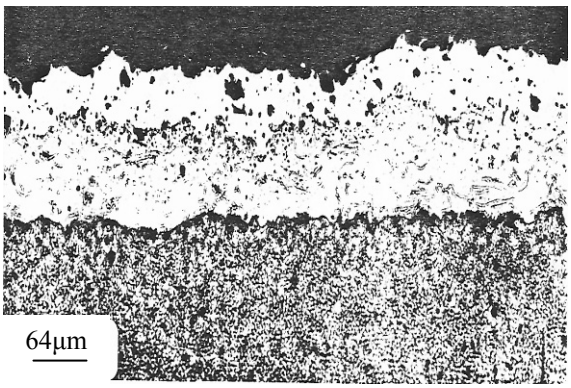

Figure 2. Cross section of the WC-Co coating

Figure 3 shows the XRD diffraction patterns of WC-Co prior and after plasma spraying. The as received WC–Co powder consists of WC and Co phases and also contained some amount of W_3Co_3C. The as-sprayed WC–Co coating includes W_2C peaks, indicating that the WC has been decarburised into W_2C under the present APS conditions. No Co or free C phases were indicated in the XRD spectrum of the coating, probably implying that their presence was in amorphous state, lacking long-range order [17]. The decarburization process is the following:

$W_2C+C \leftrightarrow 2WC$

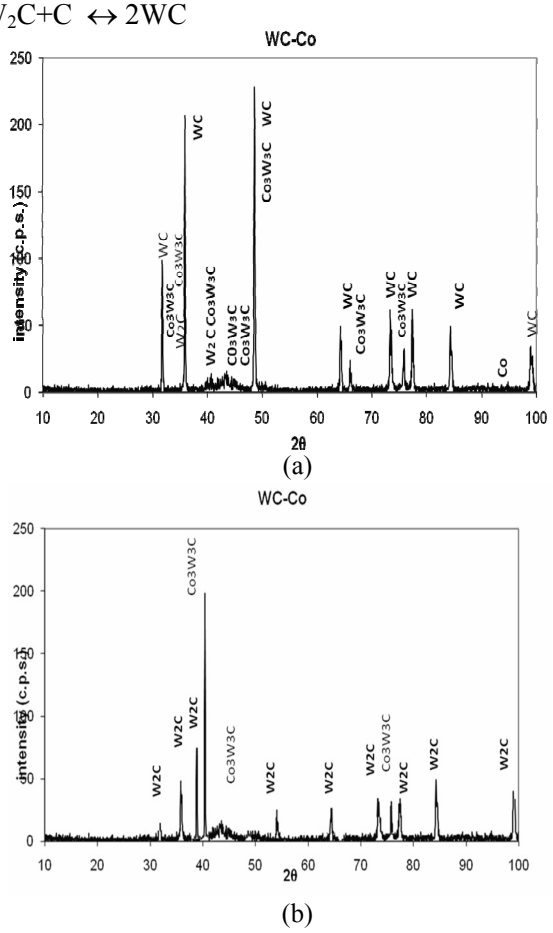

Figure 3. XRD patterns of WC-Co powder prior (a) and after (b) plasma spraying

For the decarburization of WC during the spraying process, a model has been proposed that accounts for the microstructure features observed in the coatings [18]. According to this model decarburization involves melting of cobalt during the spray process, dissolution of WC into the molten cobalt, loss of carbon from the periphery of the particles through oxidation, which thus promotes further WC dissolution locally, and quenching of the particles which results in the formation of an amorphous binder phase, and precipitation of W_2C or W depending on the degree of decarburization.

Figure 4 shows the corrosion potential of the coated and uncoated specimens as a function of immersion time. It can be seen that voltage is moving towards more negative values indicating corrosion of the system. The corrosion rate of the coated steel is lower indicating protection of the WC-Co to the steel substrate. Steel behaviour in chlorine rich environments can be described as follows [19]:

$Fe + H_2O \rightarrow FeOH + H^+ + e$
$FeOH + Cl^- \rightarrow FeCl + OH^-$
$FeCl \rightarrow Fe_2^+ + Cl^- + e^-$
$H^+ + e \rightarrow Hads$
$H_{ads} + H^+ + e \rightarrow H_2$
$2H_{ads} \rightarrow H_2$

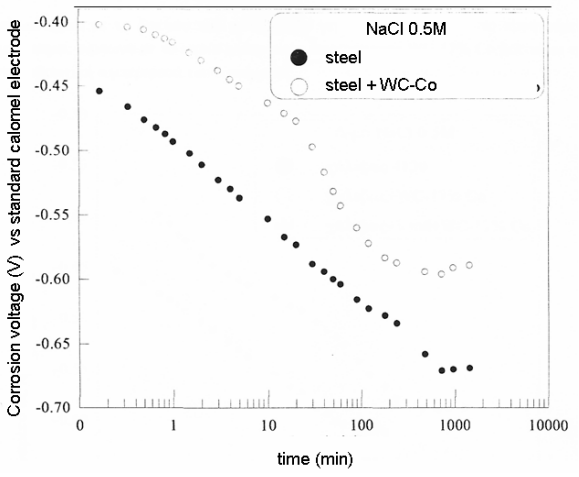

Figure 4. Corrosion voltage as a function of time for coated with WC-Co and uncoated steel

Figure 5 shows the engineering stress – strain curves for the WC-Co coated steel substrate with various coating thickness. During tensile testing the coating stared cracking at the end of elastic strains and suffered spalling just after the yield point. The experimental results show that the WC-Co plasma spray coating weakens the steel substrate in the elastic region.

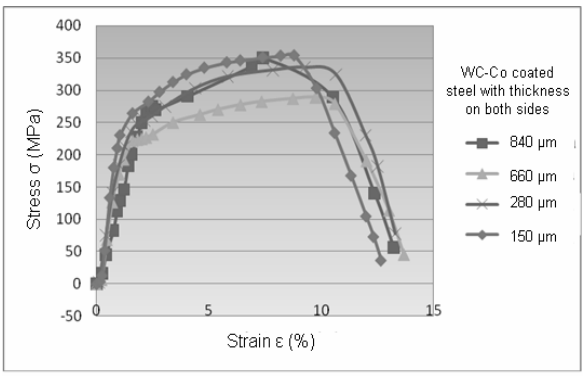

Figure 5. Stress – strain curves of WC-Co coated steel with various thicknesses

Figure 6 shows the dependence of elastic modulus on the coating thickness. It can be noted that the elastic modulus of the coated system decreases drastically with respect to the theoretical calculations as coating thickness increases. This phenomenon may be explained by the fact that the coated component behaves as a laminated composite structure stressed parallel to the lamellas with the coating and the substrate being the constituents, which determine the elastic and elastic-plastic behaviour. Simple rule of mixture approaches should be applicable in order to describe Young's modulus [20]:

$$E_{cs} = V_c * E_c + V_s * E_s \quad (2)$$

E_{cs} is the Young modulus of the coated system, V_c, V_s are the volume fractions of the coating and the substrate and E_c, E_s are the elastic modulus of the coating and the substrate in the composite system. In table 3 the experimental values of E_{cs} are listed and compared with the theoretical values calculated from equation (2) assuming that E_c = 300 GPa and E_s = 207 GPa [21].

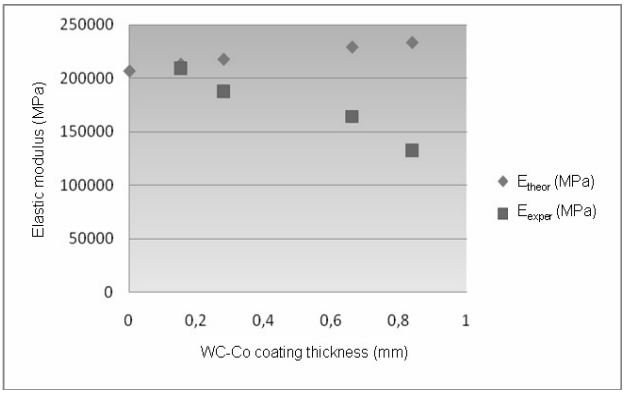

Figure 6. Elastic modulus of the WC-Co coated steel as a function of the coating thickness

It can be observed that there is a tendency agreement between the theoretical and experimental values of the Young modulus. The mean difference of the theoretical and experimental is 21% and it may be attributed to the residual stresses, which are developed during cooling and depend upon the different thermal expansion coefficients of the coating (a_c=4.6 x 10^{-6} cm/cm^{o}C) and the substrate (a_s= 11.3 x 10^{-6} cm/cm^{o}C) and can be calculated according to [22]:

$$\sigma_{rc} = E_c \Delta a \Delta T \cdot \frac{1}{1 - v_c} \quad (3)$$

where σ_{rc} are the residual stresses, Ec is the elastic modulus of the coating, v_c is the Poisson's ratio of the coating and ΔT is the temperature gradient during coating formation. Assuming v_c = 0.33 and ΔT= 400^{o}C the mean residual stresses of the WC-Co coating were calculated to be equal to 1200 MPa.

Table 3: Experimental and theoretical values of the elastic modulus

Total thickness (mm)	Coating thickness (mm)	V_s	V_c	E_{theor} (MPa)	E_{exper} (MPa)
2,2606	0,1524	0,932	0,067	213.270	209.100
2,9464	0,8382	0,715	0,284	233.457	132.400
2,7686	0,6604	0,761	0,238	229.183	164.100
2,3876	0,2794	0,883	0,117	217.883	187.500

The tribological characterization of the WC-Co coatings was intended to include the measurement of friction coefficient and the calculation of wear rate in relation to normal loads applied. Figure 7 shows representative plots for the variation of friction coefficient with sliding distance (or equivalently, time) for WC-Co coatings. Typical patterns, in general, were revealed. A running-in stage was identified in all cases examined; being more profound with the use of IC 3028 pin. During this period the value of the friction coefficient is increasing, probably due to high adhesive micro-contacts between the mating surfaces of the tribocouples [23], leading to a "peak" initial value which, however, cannot be related monotonously with the applied load.

For WC-Co coatings it is difficult to suggest a definite wear mechanism. Microscopic observations on the wear tracks revealed the existence of successive parallel sliding lines indicating an abrasion type wear (microploughing and polishing). However, taking into account the testing conditions, the wear of the counterparts (cutting insert pins) and the similar hardness of tested WC-Co disc and counterpart, a superimposed mechanism based on adhesion could be suggested [24]. This frictional behaviour could be attributed to the surface integrity state of the coating (roughness, hardness, microstructure, residual stresses) combined with a three-body (coating-wear debris-counterpart tip) dynamic contact. Moreover, the wear rate was very high at the initial stage (sliding distance < 200 m) becoming thereafter mild, indicating a possible transition of wear mechanism. After testing, a cyclic wear track was clearly shown in WC-Co disc. Regions where parts of the coating are fallen off by delamination, together with grooves, were observed on the worn WC-Co surface, indicating a prominent abrasive wear model.

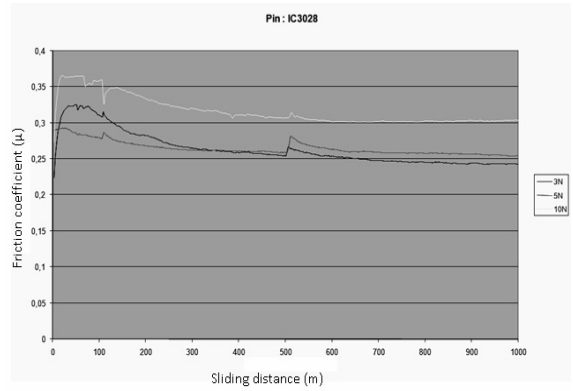

(a)

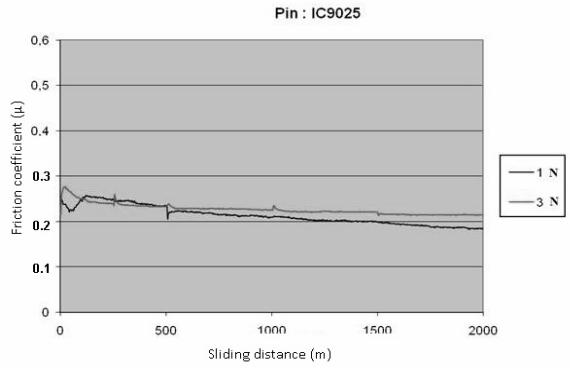

(b)

Figure 7. Representative plots for the variation of friction coefficient with sliding distance for WC-Co coatings; (a) IC 3038 and (b) IC 9025 pins

4 CONCLUSION

From the experiments presented in this paper the following conclusions can be drawn regarding the wear and corrosion resistance of WC-Co coatings:

1. WC-12% Co coatings were deposited by atmospheric plasma spray on the surface of mild steel specimens in various thicknesses. The morphology of the coating revealed porosity (3%), rough surface topography (R_a=8.2 μm) and surface hardness of 1038 HV.
2. XRD analysis of the coating revealed that the coating consists of significant quantities of W_2C attributed to decarburization of WC during spraying.

3. The WC-Co coating protects the steel substrate in chlorine rich environment.
4. The WC-Co coating decreases the mechanical strength of the steel substrate. The elastic modulus of the WC-Co coated steel decreases proportionally with the coating thickness. Differences between theoretical and experimental values of the elastic modulus may be attributed to residual stresses. These residual stresses are developed during cooling and depend upon the different thermal expansion coefficients of the coating and the substrate.
5. During wear tests a running-in stage was identified during which the friction coefficient was increasing, due to high adhesive micro-contacts between the mating surfaces of the tribocouples leading to a "peak" initial value which was not related with the applied load.

REFERENCES

[1] C. Della Corte, H. E. Sliney: Composition optimization of self-lubricating chromium-carbide-based composite coatings for use to 760 oC, ASLE Transactions, Vol. 30, No 1, pp. 77-83, 1987.

[2] K. Holmberg, H. Ronkainen, A. Matthews, in: *Proceedings of 1rst Tribology Congress on New Directions in Tribology*, Institute of Mechanical Engineers, London, Paper 251, 1997.

[3] K. Miyoshi: Lubrication by diamond and diamond like carbon coating, ASME Transactions - Journal of Tribology, Vol. 120, pp.379-384, 1998.

[4] A. Voevodin, J. O'Neill, J. Zabinski: Tribological performance and tribochemistry of nanocrystalline WC/amorphous diamond-like carbon composites, Thin Solid Films, Vol. 342, pp. 194-200, 1999.

[5] K. Brookes: World dictionary and handbook of hard metals. Int. Carbide Data, 4th ed., 1987.

[6] X.L. Jiang, F. Gitzhofer M.I. Boulos, R.Tiwari: Reactive deposition of tungsten and titanium carbides by induction plasma, Journal of Material Science, Vol. 30, pp. 2325-2329, 1995.

[7] T. Rhys-Jones: Thermally sprayed coating systems for surface protection and clearance control applications in aero engines, Surface and Coatings Technology, Vol. 43-44, No 1, pp. 402–415, 1990.

[8] B. Bourgoin, F. Mortier, in: *Proceedings of the 10th International Thermal Spraying Conference*, Essen, pp. 236-241, DVS Verlag, 1983.

[9] C Verdon., A. Karimi, J. Martin: A study of high velocity oxy-fuel thermally sprayed tungsten carbide based coatings. Part 1: Microstructures, Materials Science & Engineering A, Vol. 246, No. 1-2, pp. 11-24, 1998.

[10] B. Kear, G. Skandan, R. Sadangi: Factors controlling decarburization in HVOF sprayed nano-WC/Co hardcoatings, Scripta Materiala, Vol. 44, No 8-9, pp. 1703-1707, 2001.

[11] D. Stewart, P. Shipway, D. McCartney: Influence of heat treatment on the abrasive wear behaviour of HVOF sprayed WC–Co coatings, Surface & Coatings Technology, Vol. 105, No 1-2, pp. 13-24, 1998.

[12] H. Lia, K Khor, L. Yua, P. Cheang: Microstructure modifications and phase transformation in plasma-sprayed WC–Co coatings following post-spray spark plasma sintering, Surface & Coatings Technology, Vol. 194, pp. 96-102, 2005.

[13] Y. Qiao, T. Fischer, A. Dent: The effects of fuel chemistry and feedstock powder structure on the mechanical and tribological properties of HVOF thermal-sprayed WC–Co coatings with very fine structures, Surface & Coatings Technology, Vol. 172 pp. 24-41, 2003.

[14] Y. Ding, Y. Zhang, D. Northwood, A. Alpas: Nanoindentation and friction studies on Ti-based nanolaminated films, Surface and Coatings Technology, Vol. 89, No 1-2, pp. 24-30, 1997.

[15] N. Ak, C. Tekmen, I Ozdemir, H. Soykan and E. Celik: NiCr coatings on stainless steel by HVOF technique, Surface & Coatings Technology, Vol.174-175, pp. 1070-1073, 2003.

[16] M. Toparli, F. Sen, O. Culha, E. Celik: Thermal stress analysis of HVOF sprayed WC–Co/NiAl multilayer coatings on stainless steel substrate using finite element methods, Journal of Materials Processing Technology, Vol. 190, Issues 1-3, pp. 26-32, 2007.

[17] V. Zhitomirsky, U. Wald, S. Factor, M. Rabani, R. Zoler , S Cuperman, C. Bruma, I. Roman: WC-Co coatings deposited by the electro-thermal chemical spray method, Surface & Coatings Technology, Vol. 132, pp. 80-88, 2000.

[18] D. Stewart, P. Shipway, D. McCartney: Microstructural evolution in thermally sprayed WC–Co coatings: comparison between nanocomposite and conventional starting powders, Acta Materialia, Vol. 48, No 7, pp. 1593-1604, 2000.

[19] N. Smart, J. Bockris: Effect of water activity on corrosion, Corrosion, Vol. 48, pp. 277-280, 1987.

[20] R. Jones: *Mechanics of composite materials,* McGraw Hill, 1975.

[21] M. Watanabe, A. Owada, S. Kuroda and Y. Gotoh: Effects of WC size on interface fracture toughness of WC-Co HVOF sprayed coatings, Surface and Coatings Technology Vol. 201, pp. 619-627, 2001.

[22] H. Grunling, K. Schneider, L. Singheiser: Mechanical properties of coated systems, Materials Science Engineering, Vol. 88, pp. 177-189, 1987.

[23] M. Mohanty, R. Smith, M. De Bonte, J. Celis, E. Lugscheider: Sliding wear behaviour of thermally sprayed 75/25 Cr_3C_2/NiCr wear resistant coatings, Wear, Vol.198, pp. 251-266, 1996.

[24] M. Cadenas R. Vijande, H. Montes, J. Sierra: Wear behaviour of laser cladded and plasma sprayed WC-Co coatings, Wear, Vol. 212, pp. 244-253, 1997.